Full Spectral Decomposition of Ring Currents

E. Steiner,[†] A. Soncini,[‡] and P. W. Fowler*[,§]

University of Exeter, Exeter, EX4 4QD, United Kingdom, Afdeling Kwantumchemie, Departement Chemie, Katholieke Universiteit Leuven, Celestijnenlaan 200F, B 3001 Heverlee, Belgium, and Department of Chemistry, University of Sheffield, Sheffield, S3 7HF, United Kingdom

Received: June 16, 2006; In Final Form: September 29, 2006

Within the ipsocentric method for calculation of molecular magnetic response, projection of perturbed orbitals onto the virtual orbital space allows partition of induced current density into contributions from individual virtual excitations between occupied and unoccupied orbitals, enabling detailed assignment of the origin of currents in, e.g., benzene, cyclooctatetraene, borazine, coronene, and corannulene. Whereas delocalized currents in benzene and planar cyclooctatetraene are described by transitions within the valence space, localized currents in the borazine π system involve excitations outside the valence space.

Introduction

In the ipsocentric approach to molecular magnetic response theory, the origin of vector potential for calculation of the current density induced at a point $\boldsymbol{r}$ is placed at the point itself.[1−4] Compared with single- and few-origin methods, this choice has practical computational advantages of economy, accuracy, and convergence with basis size. It also has a decisive conceptual advantage: uniquely among distributed-origin methods,[5] the ipsocentric choice leads to partitioning of properties into distinct nonredundant contributions from occupied orbitals, free from occupied−occupied mixing. Within a defined set of canonical[3] or localized[6] occupied orbitals, current density maps can be assigned to groups of electrons.

The mathematical form of the ipsocentric perturbed wave function leads naturally to interpretation of computed current density maps in terms of energy differences and symmetry selection rules, i.e., to a frontier-orbital theory of ring currents.[3] Each perturbed molecular orbital in the magnetic field can be written as a double series of contributions from virtual excitations to unoccupied orbitals. One series involves excitations induced by the component of angular momentum about the field direction, and the other excitations induced by the components of linear momentum normal to the field, weighted by the reciprocal of the difference in energy between occupied and unoccupied orbitals. These "rotational" and "translational" series correspond respectively to paratropic and diatropic effects in the single-center approach.

Maps of orbital contributions obtained in this way have been useful in explaining the systematics of currents in monocycles,[4] circulenes,[7] macrocycles,[8] and many other systems. Sometimes the total current is dominated by a single allowed excitation, as in the 4π HOMO-LUMO diatropic ring current of benzene,[4] but often the selection rules permit virtual excitations within the valence space that share the same starting orbital but have different character, or single excitations with mixed translational and rotational character. Both are invoked in explanations of the induced currents in, e.g., large annulenes.[9]

A claim to explain, rather than simply compute, current density maps therefore faces two natural questions. If a given orbital current density map has a clear diatropic (or paratropic) pattern, is it correct to attribute this to a specific excitation, or is the map in reality a sum of contributions from excitations to the indefinitely large number of unoccupied orbitals of compatible symmetry? If the symmetry rules permit both translational and rotational excitations from a given occupied orbital, can we be sure that an explanation of the resulting map in terms of cancellation or cooperation of these different excitations is justified?

The ideal tool for exploration of these questions is an analysis that breaks the orbital contributions down further, into explicit contributions from virtual excitations. The present paper reports such an analysis and illustrates its use in refining our understanding of ring currents in some simple systems.

Method

"Ipsocentric" is our descriptive shorthand term for the method previously known as CTGO[1] and CTOCD-*DZ*[2]. In coupled Hartree−Fock (CHF) perturbation theory for a molecule in an external magnetic field with the ipsocentric choice of origin of vector potential, the first-order response of occupied orbital $\psi_n^{(0)}$ to the applied field $\boldsymbol{B}$ (neglecting small self-consistency corrections) is[3]

$$\psi_n^{(1)} = \psi_n^{(p)} + \psi_n^{(d)} = -\frac{1}{2}\sum_{p>N/2} \psi_p^{(0)} \frac{\langle \psi_p | \boldsymbol{l} | \psi_n \rangle}{\epsilon_p - \epsilon_n} \cdot \boldsymbol{B} + \frac{1}{2}\boldsymbol{R} \times \sum_{p>N/2} \psi_p^{(0)} \frac{\langle \psi_p | \boldsymbol{p} | \psi_n \rangle}{\epsilon_p - \epsilon_n} \cdot \boldsymbol{B} \quad (1)$$

where the transition operators $\boldsymbol{l}$ and $\boldsymbol{p}$ are one-electron angular and linear momenta, and $\boldsymbol{R}$ is a displacement from the origin, which in the CTOCD-*DZ*/ipsocentric approach is to be set equal to the electronic position after the differentiation step in the calculation of the current density.

Contributions of the different virtual excitations to second-order magnetic response properties could be calculated in the RPA formalism[10] by contraction of excitation amplitudes with

[†] University of Exeter.
[‡] Katholieke Universiteit Leuven.
[§] University of Sheffield.

10.1021/jp063760q CCC: $33.50
Published on Web 11/09/2006

appropriate perturbation operators expressed in the molecular-orbital basis. However, an equivalent procedure that avoids the expensive four-index transformation can be carried out in the atomic-orbital (AO) basis if all perturbed orbitals have been calculated by means of the CHF approximation cast in the McWeeny−Diercksen density-matrix formalism.[11]

In the SYSMO[12] implementation of the ipsocentric method, two first-order density matrices are calculated, one for perturbation by angular-momentum operators, l_α, and one for linear-momentum operators, p_α. Combination of the two functions according to eq 1 yields the total density matrix appropriate for the calculation of the induced current density at $\boldsymbol{r}$. Perturbed molecular orbitals for position $\boldsymbol{r}$ are therefore available and can be projected on the space of virtual orbitals, yielding separately the rotational and translational virtual-excitation terms in the current density.

The decomposition requires only the AO-projection of the perturbed molecular orbitals, the SCF coefficients for occupied and virtual orbitals, and the overlap matrix in the AO basis, all available from the standard ipsocentric calculation. A relatively minor modification of the SYSMO program yields this extra information.

Consider a closed-shell molecule with N electrons, and write the expansion of the nth perturbed MO $\psi_n^{(1)}$ in both the m atomic basis functions χ_s and the $(m - N/2)$ virtual MO's $\psi_p^{(0)}$ as

$$\psi_n^{(1)} = \sum_{s=1}^{m} c_{sn}^{(1)} \chi_s = \sum_{p>N/2}^{m} C_{pn}^{(1)} \psi_p^{(0)} \qquad (2)$$

where coefficients $C_{pn}^{(1)}$ are given formally by eq 1 up to a correction due to self-consistency, and coefficients $c_{sn}^{(0)}$ are obtained via a self-consistent CHF procedure. The values of the $C_{pn}^{(1)}$ can be easily obtained by projecting (2) on the virtual orbital $\psi_p^{(0)}$, to obtain

$$C_{pn}^{(1)} = \sum_{s=1}^{m} c_{sn}^{(1)} \langle \psi_p^{(0)} | \chi_s \rangle = \sum_{s,r=1}^{m} c_{rp}^{(0)}\, c_{sn}^{(1)} S_{rs} \qquad (3)$$

where $S_{rs} = \langle c_r | \chi_s \rangle$ is an element of the overlap matrix.

The global contribution from occupied orbital ψ_n to the three Cartesian components of the total current density, given by the expression

$$J_{n\alpha}^{(1)}(r) = -\frac{i\hbar e}{m}\{\psi_n^{(1)} \nabla_\alpha \psi_n^{(0)} - \psi_n^{(0)} \nabla_\alpha \psi_n^{(1)}\}, \qquad \alpha = x, y, z \quad (4)$$

can now be partitioned by means of eqs 2 and 3 into a sum over single self-consistent occupied-to-virtual orbital transitions, written as

$$J_{(n\to p)\alpha}^{(1)}(r) = -\frac{i\hbar e}{m} C_{pn}^{(1)}\{\psi_p^{(0)} \nabla_\alpha \psi_n^{(0)} - \psi_n^{(0)} \nabla_\alpha \psi_p^{(0)}\} \qquad (5)$$

In the absence of symmetry, a system with N occupied π orbitals and M empty π^* orbitals has $3NM$ excitations of potential interest. We would be swamped by the extra detail afforded by full spectral decomposition, if it were not for the fact that, at least for delocalized π systems, only a small number of excitations make significant contributions to the current density.

Various schemes for analysis of magnetic response could be envisaged: by orbital, by excitation per orbital, by diatropic and paratropic contribution per orbital or excitation, by total diatropic and paratropic contributions with respect to a given origin, and so on. Some illustrations for typical π systems are now given.

Applications

All calculations to be described followed the standard model that has been used extensively for small and medium π systems: the geometry of the molecule is optimized at the Restricted Hartree−Fock (RHF) level in a 6-31G** basis and the current density induced by a perpendicular external magnetic field is calculated in the same basis at the Coupled Hartree−Fock (CHF) level, using the ipsocentric distribution of origin of vector potential (i.e., CTOCD-*DZ*/6-31G**//RHF/6-31G**).

Plotting Conventions. The derivative of induced current density with respect to the inducing field is plotted at a height of 1 bohr above the molecular plane, using arrows to represent the in-plane component of this vector and contours to show the total modulus. An indication of overall current strength is given by j_{max}, the largest value in the plotting plane of the current density per unit inducing field; values are quoted as multiples of the benzene value of 0.08 au obtained with the same choices of plotting plane, basis, and method. Anticlockwise circulation of arrows in the plot corresponds to diatropic current and clockwise circulation to paratropic current.

Previous studies have dealt with maps of orbital contributions to current density, contributions from σ- and π-manifolds, and total induced current density. Here we will show maps for specific excitations that contribute to those totals. The systems studied are benzene, cyclooctatetraene (optimized under the constraint of planarity), and borazine, as examples of aromatic, antiaromatic, and nonaromatic monocycles, and coronene and corannulene, as examples of polycyclic molecules with more complex patterns of current.

(*i*) *Benzene.* Figure 1 shows the results of the spectral decomposition of the diatropic ring current in benzene. Benzene has three occupied bonding orbitals (a_{2u}, e_{1g}) and three empty antibonding π^* orbitals (e_{2u}, b_{2g}) in the π valence space. The doubly degenerate HOMO and LUMO pairs of orbitals can be split into "a" (symmetric) and "b" (antisymmetric) components according to their behavior under reflection in the mirror plane that intersects the molecular plane in a horizontal line in the structures shown in the figure. The current density maps for the four components $e_{1g,a} \rightarrow e_{2u,a}$, $e_{1g,a} \rightarrow e_{2u,b}$, $e_{1g,b} \rightarrow e_{2u,a}$, $e_{1g,b} \rightarrow e_{2u,b}$ of the HOMO-LUMO virtual excitation (allowed by translational but not rotational selection rules[4]) are shown in Figure 1, parts a to d.

All four maps are different in appearance, as they should be, but all share the common feature that they are individually incomplete: they show no closed current loops. Summed together, they recover the 4-electron HOMO orbital-pair contribution, which itself recovers essentially the whole of the π-electron current density map for benzene, i.e., the classic diatropic ring current (see, e.g., Figure 2 of ref 4). Maps of the HOMO $\rightarrow \pi^*$ excitations for virtual orbitals of e_{2u} symmetry outside the valence space show no significant current density, confirming that the HOMO-LUMO excitation accounts quantitatively for the diatropic ring current of benzene. No other orbitals are required. This is entirely consistent with the simplest, Hückel-based, picture where the *only* virtual excitation that contributes to the ring current of benzene is the node-increasing, translationally allowed HOMO-LUMO transition.[4]

(*ii*) (*Planar*) *Cyclooctatetraene.* Figure 2 shows the results of the spectral decomposition of the paratropic ring current in planar cyclooctatetraene (COT). In the Hückel picture of ring

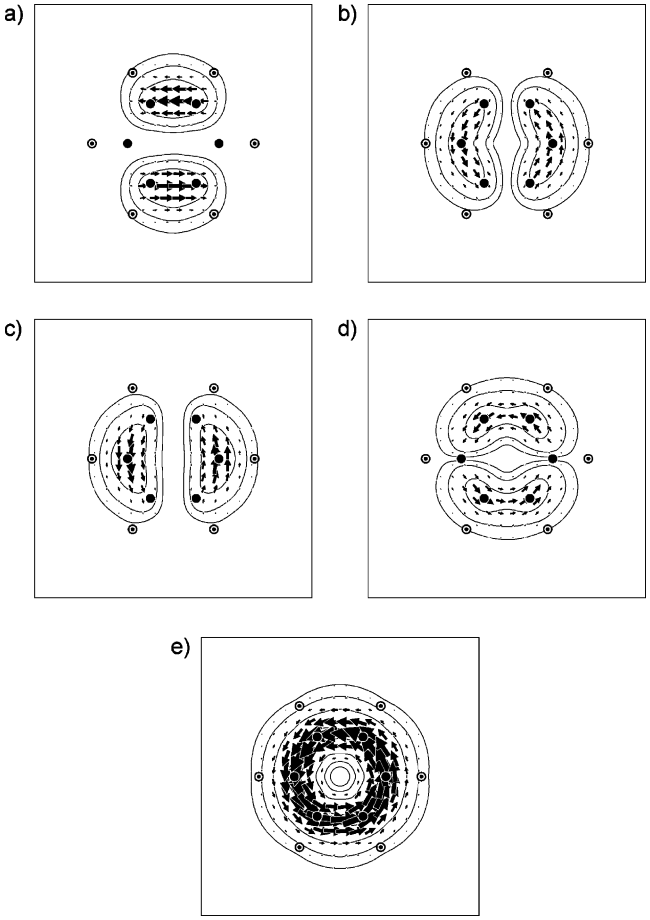

Figure 1. Current density maps computed at the RHF/6-31G**// CTOCD-*DZ*/6-31G** ipsocentric level for benzene. Panels a−d show contributions of the HOMO-LUMO virtual excitations, component to component: $e_{1g,a} \rightarrow e_{2u,a}$, $e_{1g,a} \rightarrow e_{2u,b}$, $e_{1g,b} \rightarrow e_{2u,a}$, $e_{1g,b} \rightarrow e_{2u,b}$, respectively, where subscript a (b) indicates mirror symmetry (antisymmetry) with respect to the horizontal mirror axis of the picture. Values of j_{max} are respectively 60%, 40%, 60%, and 40% of the value for benzene calculated in the same approach. Panel e shows the sum of all four contributions. Plotting conventions are described in the text.

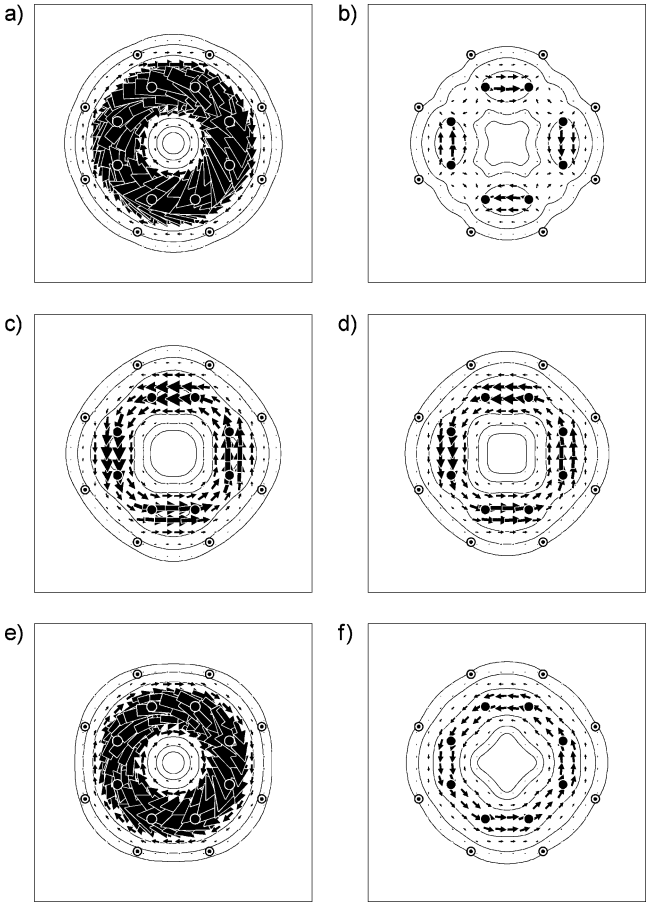

Figure 2. Current density maps computed at the RHF/6-31G**// CTOCD-*DZ*/6-31G** ipsocentric level for planar cyclooctatetrene (COT). Panels a, c), and e show the contributions of the b_{2u} HOMO, attributed to the virtual excitation to the b_{1u} LUMO (a), to the e_g LUMO+1 (c), and to the sum of these excitations (e). Panels b, d, and f analyze the contributions of the e_g HOMO-1, attributed to the virtual excitation to the b_{1u} LUMO (b), to the e_g LUMO+1 (d), and to the sum of these excitations (f). Plotting conventions are described in the text.

current of D_{4h} planarized COT there is one dominant virtual excitation, $b_{2u} \rightarrow b_{1u}$, across the small energy gap opened up by Jahn−Teller distortion from the D_{8h} symmetry of the open-shell equilateral monocycle. The small size of the gap, and the perfect rotational match between the components of the erstwhile degenerate pair ensure the dominance of the (paratropic) HOMO orbital contribution in the total π current density map, which shows only a uniform paratropic circulation.[3,4] Though dominant, this is not the only allowed virtual excitation. Symmetry also allows the HOMO to LUMO+1 excitation to contribute under the translational selection rule, but in the usual HOMO orbital map this would be masked by the strength of the paratropic excitation. Likewise, allowed excitations from the HOMO-1 to LUMO and from HOMO-1 to LUMO+1 are of opposite translational and rotational character, but are subsumed into one map when the HOMO-1 orbital contribution is computed.

Deconvolution of the different excitations confirms this Hückel-based picture in detail. The net paratropic circulation in the HOMO orbital current density map 2(e) is seen to originate from a combination of two excitation currents: an intense paratropic HOMO-LUMO excitation (Figure 2a) and a weaker but still continuous diatropic HOMO-LUMO+1 excitation (Figure 2c). Judged by comparison of j_{max} values, the paratropic excitation current is −270% of the standard benzene ring current; the diatopic excitation current is 30% of the benzene standard, and after cancellation the net paratropic current is −190% of the standard. The diatropic counter current of the HOMO-1 orbital pair (Figure 2f) (40% of the benzene standard) is seen to be dominated by the global circulation arising from virtual (diatropic) excitation to the LUMO (Figure 2d), moderated by the partial cancellation over the shorter bonds arising from the virtual (paratropic) excitation to the LUMO+1 (Figure 2b). Again, excitations to orbitals outside the valence space are not significant.

(*iii*) *Borazine.* Figure 3 shows the results of the spectral decomposition of the current density induced in borazine by a perpendicular external magnetic field. Borazine is a nonaromatic system and supports neither a diatropic nor a paratropic global ring current. The overall response of the π system is instead a pattern of local "lone-pair" circulations on the three nitrogen centers.[13] This D_{3h}-symmetric molecule has three bonding orbitals of π symmetry, spanning $a_2'' + e''$, and three antibonding orbitals, also spanning $a_2'' + e''$. A simple Huckel treatment that allows for the electronegativities of N and B indicates that the bonding orbitals will localize in N centers and the antibonding orbitals on B centers, greatly weakening global ring-current-type circulation.[14] This localization rationalizes the pictures seen in Figure 3. Excitations within the valence space

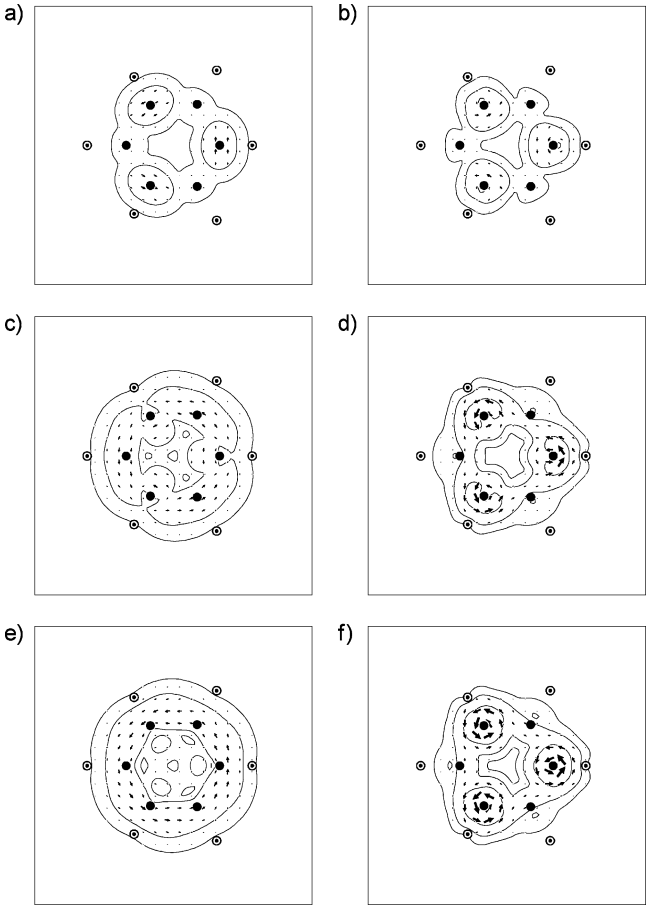

Figure 3. Current density maps computed at the RHF/6-31G**// CTOCD-*DZ*/6-31G** ipsocentric level for borazine. Panels a, c, and e show the effects on the current density arising from virtual excitations into the π* valence space from, respectively, a_2'', e'' π bonding orbitals and their $a_2'' + e''$ sum. Panels b, d, and f show the current density arising from equivalent excitations into π* virtual orbitals beyond the valence space. Plotting conventions are described in the text.

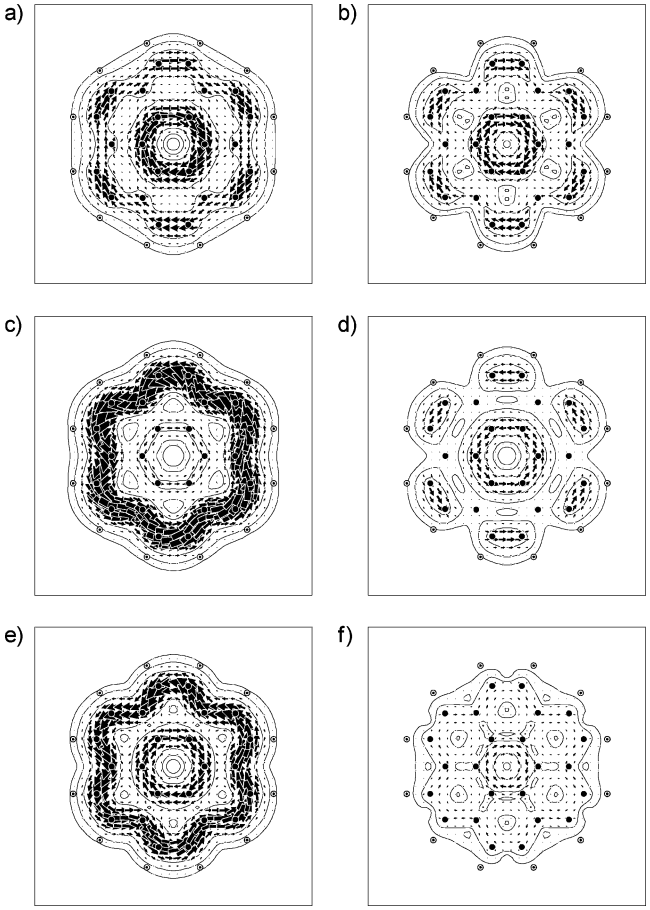

Figure 4. Current density maps computed at the RHF/6-31G**// CTOCD-*DZ*/6-31G** ipsocentric level for coronene. Panels a, c, and e depict the contribution of the e_{2u} HOMO pair: (a) the rotational $e_{2u} \rightarrow e_{2u}$ virtual excitation to the LUMO+1, (c) the translational $e_{2u} \rightarrow e_{1g}$ virtual excitation to the LUMO, and (e) their sum, yielding the characteristic [7] pattern of counter-rotating rim and hub currents. Panels b, d, and f depict the contribution of the e_{1g} HOMO-1 pair: (b) the rotational $e_{1g} \rightarrow e_{1g}$ virtual excitation to the LUMO, (c) the translational $e_{1g} \rightarrow e_{2u}$ virtual excitation to the LUMO+1, and (f) their sum. Plotting conventions are described in the text.

(Figure 3a,b) produce no significant current density. The net effect of excitations in this space is a very weak diatropic circulation, which is exactly what would be predicted by the Hückel−London model for a 6-cycle with strong alternation in electronegativity. In contrast, excitations to π* orbitals that are outside the valence space give rise to fragments of current (Figure 3b,d) that sum to a set of three concerted local circulations on nitrogen sites. Again, this is in line with semiempirical calculations with the pseudo-π model.[14] If, in such a model, each center bears only the single cylindrically symmetric orbital representing the p_π basis function, localization of currents cannot be reproduced; only when orbitals with angular nodes passing are introduced do the local current loops appear. In the present ab initio calculations, the nodes needed for the description of the first-order wave function are supplied by d basis functions; in the pseudo-π calculations they arose from in-plane p orbitals.[14] Thus, whereas delocalized currents are described by transitions within the valence space, localized currents in π systems involve excitations outside the valence space.

(*iv*) *Coronene and Corannulene.* Figures 4 and 5 show the results of the spectral decomposition of the current density induced by a perpendicular external magnetic field in the [6]- and [5]-circulenes, coronene and (planar) corannulene, respectively. Both wheel-like molecules exhibit an overall pattern of counter-rotating diatropic-rim and paratropic-hub currents.[7] Analysis of orbital contributions[3] has shown that in D_{6h} coronene both parts of the pattern arise from the HOMO e_{2u} pair, whereas in corannulene (either in the constrained D_{5h} planar form considered here or in the equilibrium bowl form) the rim and hub circulations are separately identifiable as e_1'' HOMO and e_2'' HOMO-1 contributions.

For coronene, the left-hand column of Figure 4 shows the decomposition of the HOMO contribution to current density. Under the rotational selection rule, the virtual excitation to the e_{2u} LUMO+1 supplies the central paratropic current, along with a perimeter current in the same sense (Figure 4a). Under the translational selection rule, the virtual excitation to the e_{1g} LUMO supplies the perimeter diatropic current (Figure 4c). The summed current (Figure 4e) is indistinguishable in strength (judged by j_{max}) from the paradigmatic benzene ring current. As the right-hand column of Figure 4 shows, virtual excitations from the e_{1g} HOMO-1 to the e_{1g} LUMO (rotational) and e_{2u} LUMO+1 (translational) produce canceling effects which sum to a small central paratropic circulation.

In (planar) corannulene, the picture is different in that both HOMO and HOMO-1 pairs contribute to the overall pattern of the π current density map. The contribution of the virtual excitation from e_1'' HOMO to e_1'' LUMO (Figure 5a), allowed under both rotational and translational selection rules, is a set

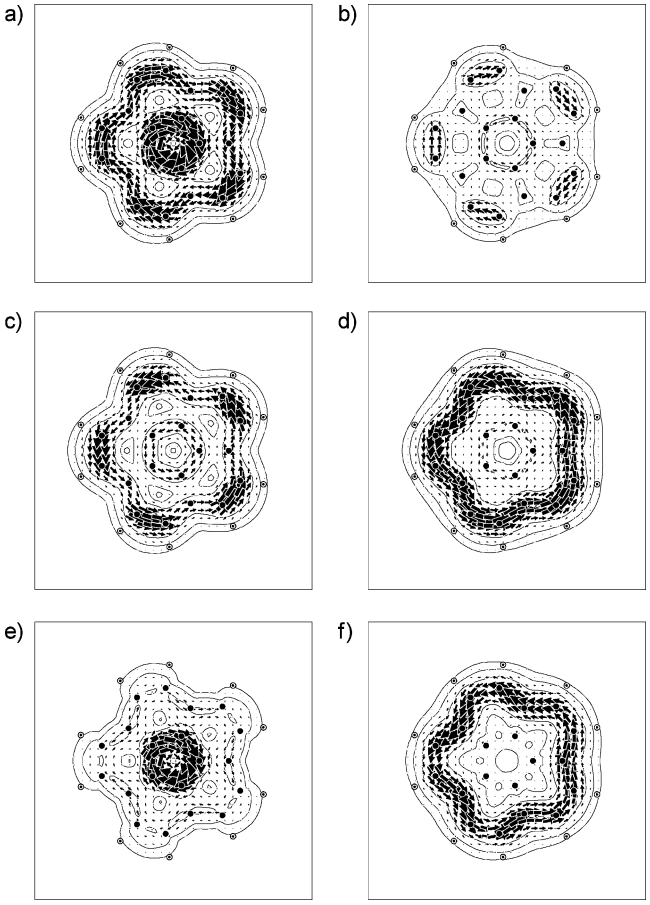

Figure 5. Current density maps computed at the RHF/6-31G**//CTOCD-*DZ*/6-31G** ipsocentric level for planar corannulene. Panels a, c, and e depict the contribution of the e_1'' HOMO pair: (a) rotational (and translational) $e_1'' \rightarrow e_1''$ virtual excitation to the LUMO, (c) summed translational virtual excitations to a_2'', a_1'', and e_2'' LUMO+1, LUMO+2, and LUMO+3, and (e) the sum of (a) and (c). Panels b, d, and f depict the contribution of the e_2'' HOMO-1 pair: (b) rotational (and translational) $e_2'' \rightarrow e_2''$ virtual excitation to LUMO+3, (d) translational $e_2'' \rightarrow e_1''$ virtual excitation to the LUMO, and (f) the sum of (b) and (d). Plotting conventions are described in the text.

of conrotating paratropic currents, consistent with the rotational rule. Excitations to the LUMO+1 to LUMO+3 (Figure 5c), all allowed under the translational selection rule, cancel out the perimeter current. The HOMO-1 e_2'' pair leads to piecewise paratropic current under the rotationally and translationally allowed virtual excitation to the e_2'' LUMO+3 (Figure 5b), whereas the translationally allowed excitation to the e_2'' LUMO (Figure 5d) produces the intense diatropic current on the perimeter that dominates the orbital contribution (Figure 5f), and has a strength (judged by j_{max}) of 95% of the benzene ring current. Summation of the two orbital contributions gives the characteristic pattern of counter-rotating rim and hub currents of corannulene.[7] Thus in polycyclic systems several excitations, both diatropic and paratropic, are necessary to describe the more complex pattern of currents.

Discussion

Spectral decomposition of induced current density has confirmed the essential correctness of the intuitive analysis of the orbital picture for ipsocentric maps for typical aromatic and antiaromatics. The diatropic ring current in benzene and the paratropic ring current of planar COT are both dominated by the contributions of HOMO-LUMO virtual excitations. The more complex patterns of current in the [*n*]-circulenes are also derived from frontier-orbital excitations that do not leave the valence space.

Although excitations beyond the valence space are unimportant for benzene, COT, and the circulenes, they are found to be essential for describing the magnetic response of borazine. The distinction between valence-space and other contributions to orbital current density maps gives an illuminating account of the source of the localized circulations.

The results for the hydrocarbons suggest that the pseudo-π method,[15] which has been used so far to model total π current and the orbital contributions to it, with good results, would also be useful for estimating the spectral breakdown of currents. Trial calculations on benzene, COT, coronene, and corannulene confirm this expectation, and the combination of pseudo-π and spectral decomposition methods is a promising one for the study of, e.g., large graphitic systems.

Finally, we note that the "spectroscopic" approach to ring current is given an extra interest by recent theoretical work on induction of periodic circulations by laser pulses. It has been proposed[16,17] that the chirality of a circularly polarized pulse may be transferred to intense unidirectional circulation of electrons on the femtosecond time scale, in what would be effectively a "real" version of the virtual excitations that figure in the ipsocentric theory of ring currents. If this can be brought to experimental realization, different transitions could be stimulated by tuning the pulses, giving the possibility of switching between patterns of current to obtain physical realizations of the component maps that are calculated within the present approach.

Acknowledgment. P.W.F. thanks the Royal Society/Wolfson Research Merit Award Scheme for support. A.S. thanks the Francqui Foundation and the Research Council of the University of Leuven for financial support.

Supporting Information Available: List of Cartesian coordinates and total energies for the five molecules treated here. This material is available free of charge via the Internet at http://pubs.acs.org.

References and Notes

(1) Keith, T.; Bader, R. F. W. *Chem. Phys. Lett.* **1993**, *210*, 223.
(2) Lazzeretti, P.; Malagoli, M.; Zanasi, R. *Chem. Phys. Lett.* **1994**, *220*, 299.
(3) Steiner, E.; Fowler, P. W. *J. Phys. Chem. A* **2001**, *105*, 9553.
(4) Steiner, E.; Fowler, P. W. *Chem. Commun.* **2001**, 2220.
(5) Steiner, E.; Fowler, P. W. *Phys. Chem. Chem. Phys.* **2004**, *6*, 261.
(6) Steiner, E.; Fowler, P. W.; Havenith, R. W. A. *J. Phys. Chem. A* **2002**, *106*, 7048.
(7) Steiner, E.; Fowler, P. W.; Jenneskens, L. W. *Angew. Chem., Int. Ed.* **2001**, *40*, 362.
(8) Steiner, E.; Fowler, P. W. *ChemPhysChem.* **2002**, *3*, 114.
(9) Soncini, A.; Fowler, P. W.; Jenneskens, L. W. *Phys. Chem. Chem. Phys.* **2004**, *6*, 277.
(10) Caves, T. C.; Karplus, M. *J. Chem. Phys.* **1969**, *50*, 3649.
(11) Diercksen, G. H. F.; McWeeny, R. *J. Chem. Phys.* **1966**, *44*, 3554.
(12) Lazzeretti, P.; Zanasi, R. SYSMO Package; University of Modena, 1980. Steiner, E.; Fowler, P. W.;. Havenith, R. W. A.; Soncini, A.: additional routines for evaluation and plotting of current density.
(13) Fowler, P. W.; Steiner, E. *J. Phys. Chem.* **1997**, *101*, 1409.
(14) Soncini, A.; Domene, C.; Engelberts, J. J.; Fowler, P. W.; Rassat, A.; van Lenthe, J. H.; Havenith, R. W. A.; Jenneskens, L. W. *Chem.-Eur. J.* **2005**, *11*, 1257.
(15) Fowler, P. W.; Steiner, E. *Chem. Phys. Lett.* **2002**, *364*, 259.
(16) Barth, I.; Manz, J. *Angew. Chem., Int. Ed.* **2006**, *45*, 2962.
(17) Barth, I.; Manz, J.; Shigeta, Y.; Yagi, K. *J. Am. Chem. Soc.* **2006**, *128*, 7043.